MINISTRY OF EDUCATION AND TRAINING
VIETNAM ACADEMY OF SCIENCE AND TECHNOLOGY

GRADUATE UNIVERSITY OF SCIENCE AND TECHNOLOGY

Nguyen Thi Ngoc Hoi

STRUCTURE-ADJUSTABLE SYNTHESIS OF HOLLOW MESOPOROUS SILICA NANOPARTICLES AND ITS SURFACE MODIFICATION FOR ANTI-CANCER DRUG DELIVERY

Major: **Polymeric And Composite Materials**

Code: **9440125**

SUMMARY OF POLYMERIC AND COMPOSITE MATERIALS DOCTORAL THESIS

Ha Noi - 2022

The dissertation was completed at Graduate University of Science and Technology - Vietnam Academy of Science and Technology

Scienctific Supervisor: Assoc. Prof. Ph.D. Nguyen Dai Hai

Reviewer 1: Assoc. Prof. Ph.D. Pham Nguyen Kim Tuyen

Reviewer 2: Assoc. Prof. Ph.D. Bach Long Giang

Reviewer 3: Assoc. Prof. Ph.D. Nguyen Thi Phuong Phong

The dissertation was defended in front of the Thesis Committee for Doctoral Degree at Graduate University of Science and Technology - Vietnam Academy of Science and Technology, at 02:00 p.m, 30th December, 2022.

The dissertation can be found at:

- Library of Graduate University Science And Technology
- Vietnam National Library

PREAMBLE

1. The urgency of the thesis

Mesoporous silica nanoparticles (MSNs) have been known to be widely studied materials for biomedical applications, especially drug delivery due to their suitable properties such as high surface area, large pore volume, adjustable pore size, high biocompatibility and easy surface modification. As a member of the MSN family, hollow mesoporous silica nanoparticles (HMSN) has a structure consisting of the outer mesoporous shell and the inner hollow cavity. Therefore, HMSN also has additional outstanding advantage that is its superior drug carrying capacity compared to MSN thanks to the hollow cavity. HMSNs can be synthesized by different methods, in which hard templating is known to be the most popular method. With hard hard templating, the three common characteristics of HMSNs that can be adjusted are hollow cavity volume, mesoporous shell thickness and mesopore diameter. Moreover, silanol groups on HMSN's surface can be easily modified with different ligands to improve the properties of HMSN-based drug delivery systems.

In this study, in order to create a silica-based nanocarrier system for anti-cancer drug delivery, the project focused on synthesizing spherical HMSN particles with the desired size in the range of 100 nm. The mesoporous shell thickness and mesopore diameter of HMSNs would be controlled using different polymers in the shell coating step to accommodate the delivery and release of different sized therapeutic agents. In addition, different pluronics would be denatured on HMSNs' surface for the enhancement of their drug loading capacity, encapsulated drug storage ability, drug release controllability and targeting ability. From the above analysis, the project "**Structure-adjustable synthesis of hollow mesoporous silica nanoparticles and its surface modification for anti-cancer drug delivery**" would contribute to perfecting the drug carrier system based on hollow mesoporous silica nanoparticles.

2. Research objectives of the thesis

Research on the synthesis of hollow mesoporous silica nanoparticles (HMSN) with the size of about 100 nm, controlable mesoporous shell thickness and mesopore diameter, as well as the modification of HMSN with Pluronics to improve the cancer cell killing efficiency of the drug carrier system.

3. The main research contents of the thesis

1. Synthesis of hollow mesoporous silica nanoparticles (HMSN) with a diameter of less than 100 nm.
2. Investigation of the influence of molecular weight and the concentration of polyethylene glycol on HMSN's mesoporous shell thickness.

3. Investigation of the influence of different non-ionic surfactants on the mesoporous shell thickness and mesopore diameter of HMSNs.
4. Modification of HMSNs' surface with different Pluronics, evaluate physico-chemical and biological properties of HMSN-Plu systems in the improvement of drug delivery and drug release control.
5. Study on the effect of dual drug encapsulation and investigation of drug release profiles of HMSN and HMSN-Plu.
6. Evaluate cytotoxicity and cancer cell killing efficiency of drug carrier systems HMSN and HMSN-Plu.

-------o0o-------

CHAPTER 1. LITERATURE REVIEW

1.1. Structure of Hollow Mesoporous Silica Nanoparticles (HMSN)

As a member of MSN family, HMSN's structure consists of two main parts, the outer mesoporous shell and the inner hollow cavity. Therefore, besides the specific properties of MSN, HMSN possesses another outstanding advantage which is its excellent drug loading capacity compared to MSN thanks to the hollow cavity inside.

1.2. Methods of HMSN synthesis

Based on the template, the methods for synthesizing HMSN are classified into three methods: soft-template, hard-template and self-template. About hard-template method, the prepared solid particles are used as cores and will be removed after the formation of mesoporous shells which are formed by the self-assemble between precusors and surfactant template.

1.3. Modular factors of HMSN

One of the outstanding advantages of HMSN, making them versatile and potential in biomedical applications is their feasibility and ease of tuning. The three most common properties of HMSNs being adjusted are cavity volume, porous shell thickness, and pore diameter.

For HMSN, it can be said that the hollow cavity is the place to store the drug and the pores are the path to help release the drug from the empty cavity inside the particles to the outside environment. Thus, adjusting the cavity volume will directly affect the drug loading capacity of HMSN. Based on the synthesis method presented in the previous section, the cavity volume of HMSN synthesized by the hard core method can be adjusted through adjusting the size of the hard core.

The mesoporous shell thickness has been reported to be one of the main factors affecting the drug release profile of HMSN particles. Therefore, modulating the mesoporous shell thickness is a potential approach to be able to fabricate HMSN materials with desired drug release profiles. Basically, the adjustment of MSN mesoporous shell thickness is similar to the control of

diameters of $dSiO_2$ and MSN particles through the reaction parameters during the sol-gel process.

An adjustable property is the pore size or pore diameter of the mesoporous shell. Normally, the MSN shell has a mesopore size of 2–3 nm, which is sufficient to transport through and carry small molecules. However, this pore diameter cannot be applied to large molecules (eg nucleic acids, peptides, proteins, …), thus limiting the function of MSNs in general and HMSNs in particular in drug delivery applications. So the researchers devoted their efforts to widening the pore diameter.

1.4. Surface-modified HMSN and dual-drug carrier HMSN

HMSN particles have shown certain limitations that need to be improved and overcome, including: (1) Open pores that cause drug to leak, (2) The silanol groups on the surface interact with the phospholipids on the cell membrane. erythrocytes lead to hemolysis. These limitations can be overcome by surface modification of HMSN.

Nanoparticles are often modified with polymers because it improves drug delivery and therapeutic efficacy. Some popular polymers are used to modify with MSN such as PEG, pluronic, dendrimer, chitosan, etc. Among them, Pluronic has been researched and applied in drug delivery systems, especially poorly soluble drugs.

Meanwhile, the trend to improve the effectiveness of chemotherapy is the use of a combination of drugs. This led to the idea of denaturing HMSN with Pluronic for dual drug delivery application, which improves the cancer cell killing efficiency of the drug delivery system.

-------o0o-------

CHAPTER 2. MATERIALS AND EXPERIMENTAL METHODS

2.1. Synthesis method of HMSN

Hollow mesoporous silica nanoparticles were synthesized through a hard-template method via three main steps. To control the HMSN particle diameter below 100 nm, the particle size of the hard template $dSiO_2$ was reduced through the synthesis components such as the concentration of silica precursor TEOS, the concentration of catalyst agent NH_3 and the amount of EtOH. Moreover, the time of mesoporous silica coating step and hard template silica etching step would be shortened through reactional parameters such as temperature and catalyst agent.

2.2. Investigation the effect of PEG on HMSN's mesoporous shell thickness

To investigate the effects of PEG on the mesoporous shell thickness of HMSN, PEG with difference molecular weight (1000, 2000, 4000 and 6000 g/mol) and weight percentage (from 1% to 5%) was added into the reaction

mixture in the second step of the synthesis process of hollow mesoporous silica nanoparticles as described in.

A part of the achieved solution after the second step was dialyzed by 12 x 14 kDa membranes against ethanol and distilled water in 3 days before being lyophilized to obtain $dSiO_2$@MSN. The post- lyophilized $dSiO_2$@MSN samples were calcined at 600 °C for 2 hours to removal of residual organic components for further experiments. These $dSiO_2$@MSN samples were measured DLS and SEM to determine the morphology and diameter of the particles. Based on the DLS particle diameter of $dSiO_2$ and $dSiO_2$@MSN, the thickness of the mesoporous shell would be calculated following the equation:

$$T_S = \frac{d_{dSiO2@MSN} - d_{dSiO2}}{2} \qquad (1)$$

Where: TS: the thickness of mesoporous shell (nm)
d_{dSiO2}@MSN: diameter of $dSiO_2$@MSN particles (nm)
d_{dSiO2}: diameter of $dSiO_2$ particles (nm)

The rest of the $dSiO_2$@MSN solution was continued to conduct the third step to obtain HMSN. The post- lyophilized HMSN samples were calcined at 600 °C for 2 hours to complete removal of residual organic components for further experiments.

2.3. Investigate the effect of non-ionic surfactants on the mesopore diameter of HMSN

To investigate the effects of non-ionic surfactants (S), including Brij S10 (BS10), Tween 20 (T20) and Tween 80 (T80) on the meso-pore diameter of HMSN, these S at difference molar ratio with the constant CTAB (0:1, 1:4, 1:3, 1:2 and 1:1) was used to prepared mixed micelles, which were used in the second step of the HMSN synthesis process as co-templates to coat the mesoporous shell onto the hard core $dSiO_2$.

A part of the achieved solution $dSiO_2$@MSN was treated as the same as described in part 2.2. Then, the samples were measured DLS size, BET and BJH. The thickness of the mesoporous was calculated based on the particle diameter of $dSiO_2$ and $dSiO_2$@MSN and the equation (1). Based on the BET and BJH analysis, the meso-pore diameter of $dSiO_2$@MSN samples were determined and compared. The rest of the $dSiO_2$@MSN solution was continued to conduct the third step to obtain HMSN and the products were characterized via SEM, TEM, Zeta potential, XRD and FT-IR analysis.

2.4. Study on the modification of HMSN with Pluronics

The HMSN surface is first modified with an amine group through 3-aminopropyltriethoxysilane (APTES) to produce the product HMSN-NH_2. The pluronics are activated by 4-Nitrophenyl chloroformate (NPC) to form NPC-Plu-

OH. Because NPC easily reacts with amine groups in water, HMSN-NH_2 is reacted with NPC-Plu-OH in aqueous medium to produce HMSN-Plu.

2.5. Study on the encapsulation effect of the nano carriers

To evaluate the drug encapsulation capacity of the hollow silica nanoparticles and surface functionalized samples, the membrane diffusion method was used. Drug loading efficacy - DLE (Drug loading efficacy) and drug carrying capacity - DLC was determined following the equations:

$$DLE\ (\%) = \frac{20 - W_{non\text{-}D}}{20} \times 100\% \qquad (2)$$

$$DLC\ (\%) = \frac{20 - W_{non\text{-}D}}{(W_{particles} + 20 - W_{non\text{-}D})} \times 100\% \qquad (3)$$

Where: 20 (mg) was the initial drug amount

$W_{non\text{-}D}$ was the mass of unloaded drug (mg)

$W_{particles}$ was the mass of nano carrier (mg)

2.6. Investigation of drug release rate of the nano carriers

The PBS buffer is an isotonic solution with pH 7.4 similar to the pH in the human body. The pH level of cancer cells which is at 5.5 is a typical solution for dialysis of biocompatibilities. The membrane dialysis method was used to investigate the slow release of drug from the carrier system.

2.7. Study on cytotoxicity of the nano carriers

The MTT method was employed to evaluate the cytotoxicity of the drug carrier system and the effect of killing cancer cells of the carrier system when carrying anti-cancer drugs. The MCF-7 and Hela cell lines were used in the evaluation process.

2.8. Characterization methods of the nano carriers

Material morphology and surface were examined by SEM and TEM. Particle size, particle size distribution, zeta potential were evaluated through DLS. The XRD spectroscopy was then applied to analyze the structure and spatial characteristics of the material. Subsequently, the method of FT-IR was used to analyze functional groups, identify organic compounds and study the structure of the material. To evaluate the surface area and pore volume, the N_2 gas adsorption - desorption method was used.

-------o0o-------

CHAPTER 3. A MODIFIED HARD-TEMPLATING FOR HOLLOW MESOPOROUS SILICA NANOPARTICLES SYNTHESIS WITH SUITABLE PARTICLE SIZE AND SHORTENED SYNTHESIS TIME

3.1. Etching over time of silica hard-template in the synthesis of hollow mesoporous silica nanoparticles

The obtained $dSiO_2$ particles are mono-disperse spheres with zeta potential of -45.8 mV, DLS size of 96.8 nm and TEM size of 65.3 ± 0.4 nm.

HMSN particles which was under different etching time from 30 to 180 minutes were taken SEM and TEM image (Figure 3.2). The images presented that the particles had non-hollow core structure after 30 and 60 minutes of etching. The hollow core structure of HMSN was visible after 90 minutes and most obvious after 120 minutes of etching. However, after 150 minutes of etching, the shell appeared to have some holes in it, indicating that it had begun to be corroded but the particles was still spherical. Finally, after 180 minutes of etching, the particles lost their spherical shape and the shell was collapsed. These results suggested that the suitable etching time was 120 minutes, consequently the HMSN 120 would used for further experiment.

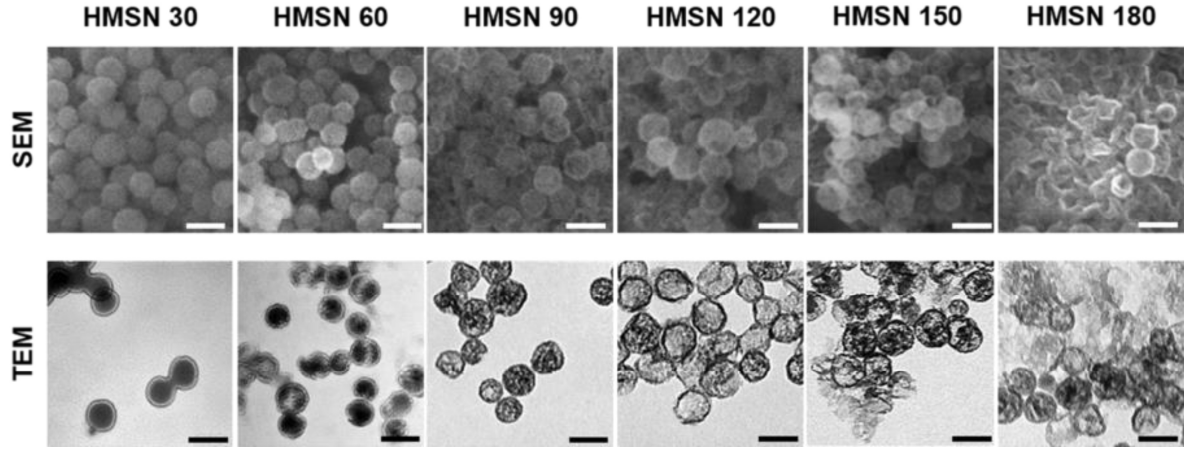

Figure 3.2. SEM and TEM images of HMSN over etching time. Scale bar = 100 nm.

The synthesis time of HMSN in the current study decreased from 21 hours to 9 hours. In details, hard-template preparation time was remained for 6 hours, mesoporous shell coating time shortened to 1 hour and hard-template etching time shortened to 2 hours. This modified hard-template method with shorter synthesis time would be meaningful for scientists who study on silica nanoparticles as well as for industrial scale production.

3.2. Characterizations of synthesized HMSN

The synthesized HMSN particles were characterized via TEM, BET, and BJH (Figure 3.3). TEM images HMSN 120 clearly showed the hollow@shell structure of the particles with the particle diameter of 80.2 ± 1.29 nm, the hollow diameter of 65.3 ± 0.95 nm, and the mesoporous shell thickness of about 7.5 nm. Compare to the previous studies, the particle size of the synthesized HMSN reduced from over 134 nm to about 80 nm. The HMSN's isotherms was classified as Langmuir type IV isotherm curve and type H_2 hysteresis loop according to IUPAC. proving

mesoporous nature of the synthesized HMSN. Additionally, the surface area and the pore diameter of HMSN were determined as about 767 m^2/g and 2.5 nm, respectively.

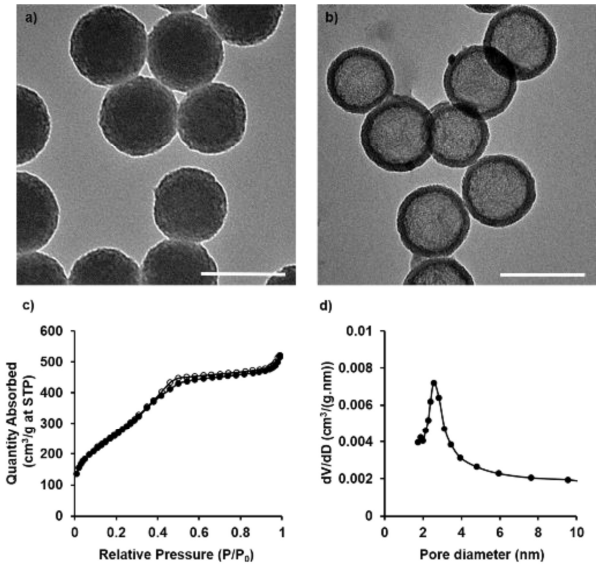

Figure 3.3. a) TEM image of $dSiO_2$@MSN; b) TEM image of HMSN; c) N_2 adsorption and desorption of HMSN; d) Pore size distribution of HMSN. Scale bar = 100 nm.

In addition, FT-IR, EDX, Zeta, DLS, TGA, XRD and MTT analyzes were performed to characterize and evaluate the biocompatibility of HMSN particles.

-------o0o-------

CHAPTER 4. SIMPLY AND EFFECTIVELY CONTROL THE SHELL THICKNESS OF HOLLOW MESOPOROUS SILICA NANOPARTICLES BY POLYETHYLENE GLYCOL FOR DRUG DELIVERY APPLICATIONS

4.1. Effect of PEG molecular weight on the mesoporous shell thickness of dSiO2@MSN

PEG with molecular weights of 1000, 2000, 4000 and 6000 g/mol was added 3% (w/v) into the reaction mixture. The obtained samples named $dSiO_2$@MSN-P1k, $dSiO_2$@MSN-P2k, $dSiO_2$@MSN-P4k and $dSiO_2$@MSN-P6k were determined DLS size and SEM images (Figure 4.1).

The samples including hard template $dSiO_2$, $dSiO_2$@MSN and $dSiO_2$@MSN-Pxk (x was 1, 2, 4 and 6) were obtained with spherical shape, monodisperse, and highly narrow size distribution. In addition, SEM images showed that $dSiO_2$ particles had clear boundaries and fine surface. Meanwhile, $dSiO_2$@MSN and $dSiO_2$@MSN-Pxk particles performed less clear boundaries and slightly rough

surface. This suggested that mesoporous shell had been successfully coated on the hard template $dSiO_2$.

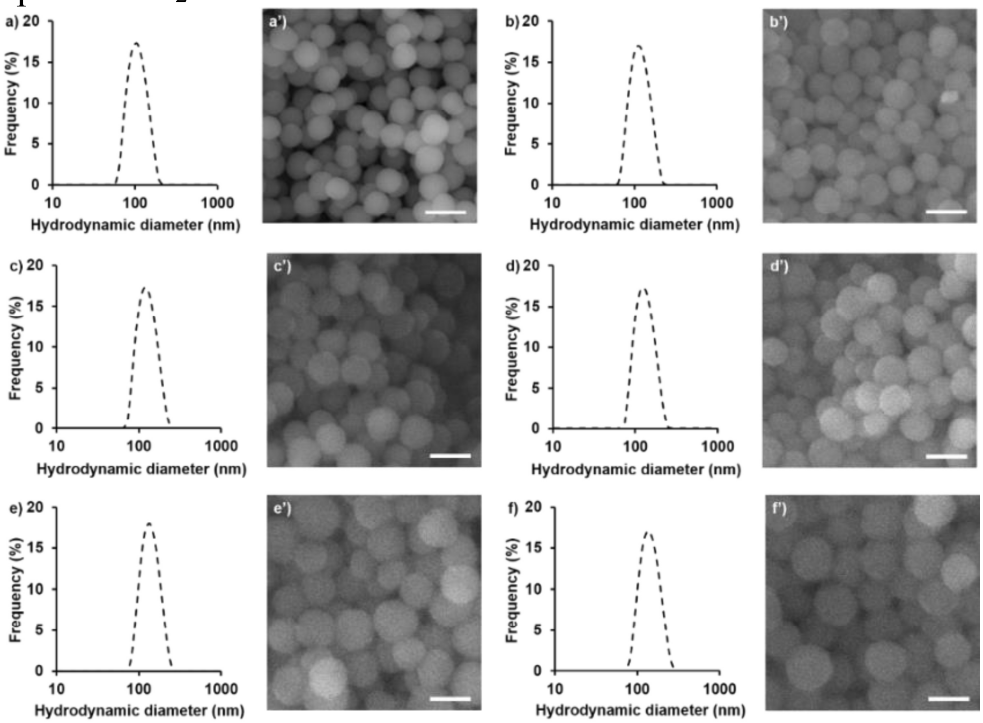

Figure 4.1. DLS size and SEM images of $dSiO_2$ (a, a'), $dSiO_2$@MSN (b, b'), $dSiO_2$@MSN-P1k (c, c'), $dSiO_2$@MSN-P2k (d, d'), $dSiO_2$@MSN-P4k (e, e') and $dSiO_2$@MSN-P6k (f, f'). Scale bar = 100 nm.

At the same concentration of PEG (3%, w/v) in the reaction mixture, when PEG molecular weight increased from 1000 to 6000 g/mol, the mesoporous shell thickness gradually increased from 6.90 nm to 16.20 nm, respectively. However, there was no statistically significant difference between the pairs $dSiO_2$@MSN versus $dSiO_2$@MSN-P1k, $dSiO_2$@MSN-P1k versus $dSiO_2$@MSN-P2k, and $dSiO_2$@MSN-P4k versus $dSiO_2$@MSN-P6k ($p < 0.05$).

For HMSNs with the same cavity volume, which one has a thicker mesoporous shell is expected to have more space for drug encapsulating and more sustained drug release profile. Moreover, in order to ensure a certain mechanical stability for HMSNs, they should have a sufficiently thick mesoporous shell so as not to break during handling and administration. According to Lasio et al., HMSNs with shell thickness from 14 to 18 nm with complete shells were broken under pressure from 103.0 to 123.6 MPa. Therefore, HMSN particles in the current study with mesoporous shell thickness in the range of 14.40 to 16.20 nm, which were obtained in the presence of 3% (w/v) PEG 4000 and PEG 6000, were expected to meet the above mentioned characteristics. PEG 6000 was chosen to prepare HMSN for further studies.

4.2. Effect of PEG weight percentage on the mesoporous shell thickness of $dSiO_2$@MSN

PEG 6000 was added into the reaction mixture with difference amount from 1% to 5% (w/v). The obtained samples named $dSiO_2$@MSN-Py% (y was from 1 to 5) were determined DLS size and SEM images (Figure 4.2). When the concentration of PEG 6000 increased from 1% to 5% (w/v), the mesoporous shell thickness corresponding increased from 10.45 to 18.25 nm. These results once again confirmed that the presence of PEG in the reaction system would increase the mesoporous shell thickness of HMSN particles. However, there was no statistically significant difference between the samples $dSiO_2$@MSN-P2%, $dSiO_2$@MSN-P3%, $dSiO_2$@MSN-P4% and $dSiO_2$@MSN-P5%.

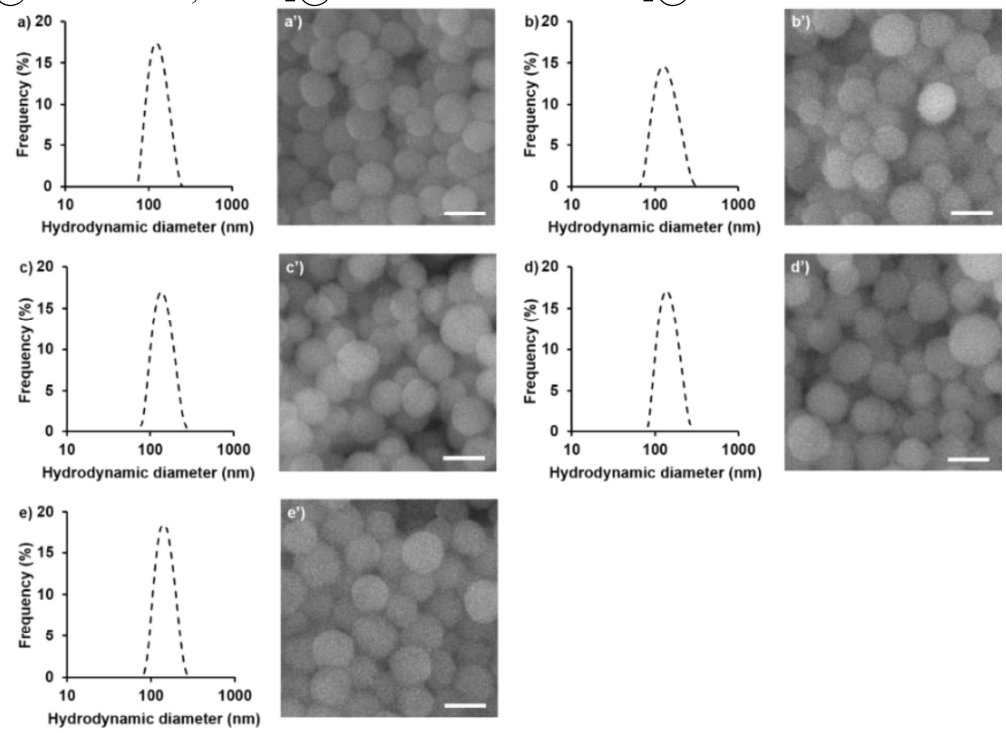

Figure 4.2. Size dispersion by dynamic light scattering (DLS) measurement and field-emission scanning electron microscopy (FE-SEM) images of $dSiO_2$@MSN-P1% (a, a'), $dSiO_2$@MSN-P2% (b, b'), $dSiO_2$@MSN-P3% (c, c'), $dSiO_2$@MSN-P4% (d, d') and $dSiO_2$@MSN-P5% (e, e'). Scale bar = 100 nm.

In aqueous solution, ether oxygen atoms of PEG (−O−) formed hydrogen bonds with water molecules. Therefore, separate zigzag chains of PEG through hydrogen bonds with water molecules would form an ordered net structure. At the same concentration in the reaction system, the higher the PEG molecular weight is, the more enlarged the PEG net structure horizontally is. Meanwhile, when the concentration in the reaction system of the same PEG increases, its ordered net

structure will expand vertically. When the amount of PEG added is greater than the saturation adsorption of the nanoparticles in solution, this ordered net structure could change the particle growth kinetics which promotes nucleation and facilitates the particle agglomeration. Therefore, growing the PEG network in the solution either vertically (increase the PEG concentration) or horizontally (increase the PEG molecular weight) could promote the nucleation and agglomeration of silica nanoparticles. This explained the result that the mesoporous shell thickness increased as the PEG molecular weight or the PEG concentration in the reaction system increased. However, with a specific amount of TEOS precursors and under a determined reaction conditions, to a certain limit, continuing to increase PEG molecular weight or PEG concentration could not further enhance the nucleation and agglomeration of the nanoparticles. This result was consistent with the previous publications about the role of PEG on nanoparticle crystallization.

Based on the calculated mesoporous shell thickness and statistical analysis, PEG 6000 at the concentration of 2% (w/v) was selected to synthesize HMSN for further experiments. In order to better evaluate the role of PEG on the properties of the synthesized HMSN materials, the obtained particles with the presence of PEG in the synthesis – HMSN-P2% would be characterized in the comparison with HMSN-0.

4.3. Characterizations of the synthesized HMSNs

The synthesized HMSN particles with and without the presence of PEG were characterized via TEM and Zeta potential (Figure 4.4).

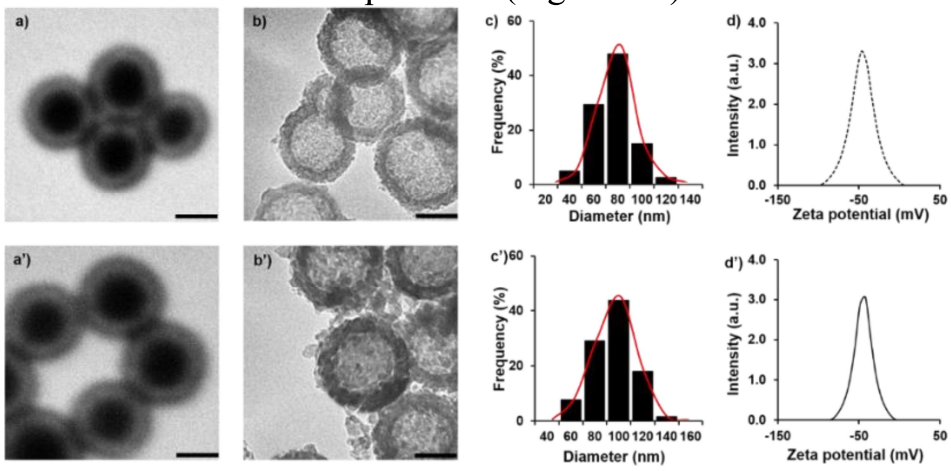

Figure 4.4. Characterizations of the synthesized silica nanoparticles: TEM images of $dSiO_2$@MSN-0 (a) and $dSiO_2$@MSN-P (a'); TEM images (b and b'); Size distribution (c and c'); Zeta potential (d and d') of HMSN-0 and HMSN-P, respectively. Scale bar = 50 nm.

Both $dSiO_2$@MSN and HMSN samples with and without PEG were morphologically monodispersed spherical particles. Statistical results based on TEM images using ImageJ showed that the HMSN-0 particles had a diameter of 80.2 nm and a mesoporous shell 7.5 nm thick, while the HMSN-P had a diameter of 94.3 nm and a 14.5 nm thick mesoporous shell. This result was quite consistent with the results presented in section 3.2, which was calculated based on DLS size and Equation (1). In addition, zeta potential of both HMSN-0 and HMSN-P had negative values near -50 mV, indicating that PEG was well removed from the synthesized HMSN-P samples.

4.4. Drug loading and in vitro drug release study of the synthesized HMSNs

DLE and DLC values of HMSN-P lightly lower than HMSN-0's one. However, there was no statistical difference of DLC and DLE between the two samples ($p < 0.05$). This result showed that although the mesoporous shell thickness increased when synthesized in the presence of PEG, the drug loading capacity of HMSN materials was still maintained.

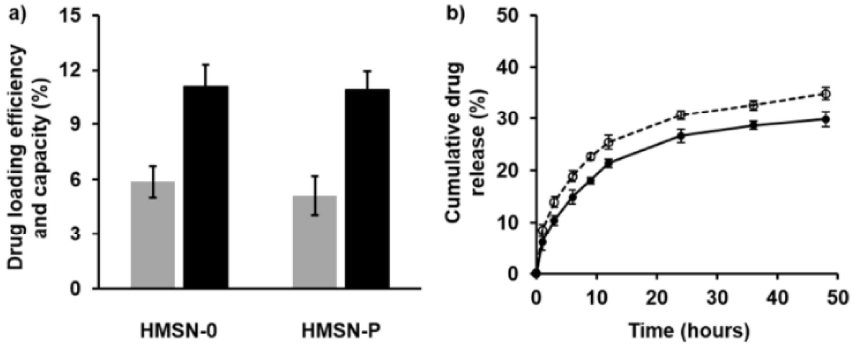

Figure 4.7. DOX loading capacity (DLC - grey) and DOX loading efficiency (DLE - black) of HMSN-0 and HMSN-P (a); In vitro release profile of Dox@HMSN-0 (empty circle) and Dox@HMSN-P (solid circle) (b). The marked points correspond to 0, 1, 3, 6, 9, 12, 24, 36 and 48 h, respectively.

Both HMSN-0 and HMSN-P showed sustainable release profiles with no more than 35% of the initial DOX was released by each within 48 h. Though, from the 12-hour mark onwards, the amount of drug released from HMSN-P was about 4-5% lower than from HMSN-0. This suggested that HMSN-P with similar loaded drug but longer meso-channels exhibited better controlled release pattern compared to HMSN-0. The reason for this might be that the drug took longer to move through the longer meso-channels to the outside.

In addition, BET, BJH, FT-IR, EDX and MTT analyzes were performed to characterize and evaluate the biocompatibility of HMSN particles.

-------o0o-------

CHAPTER 5. NON-IONIC SURFACTANTS AS CO-TEMPLATES TO CONTROL THE MESOPORE DIAMETER OF HOLLOW MESOPOROUS SILICA NANOPARTICLES FOR DRUG DELIVERY APPLICATIONS

5.1. Effect of non-ionic surfactants on the mesoporous shell thickness of $dSiO_2$@MSN

To investigate the effect of Tween 20, Tween 80 and Brij S10 in mixed micelles on the mesoporous shell thickness of $dSiO_2$@MSN, mixed micelles of the three non-ionic surfactants with CTAB at different molar ratios were used as co-templates in the shell coating step. The obtained samples $dSiO_2$@MSN-S were determined DLS size (Figure 5.2). Based on the DLS diameter of $dSiO_2$ (reported as 96.8 ± 1.99 nm in the previous publication), $dSiO_2$@MSN and $dSiO_2$@MSN-S, the mesoporous shell thickness was calculated using the equation (1).

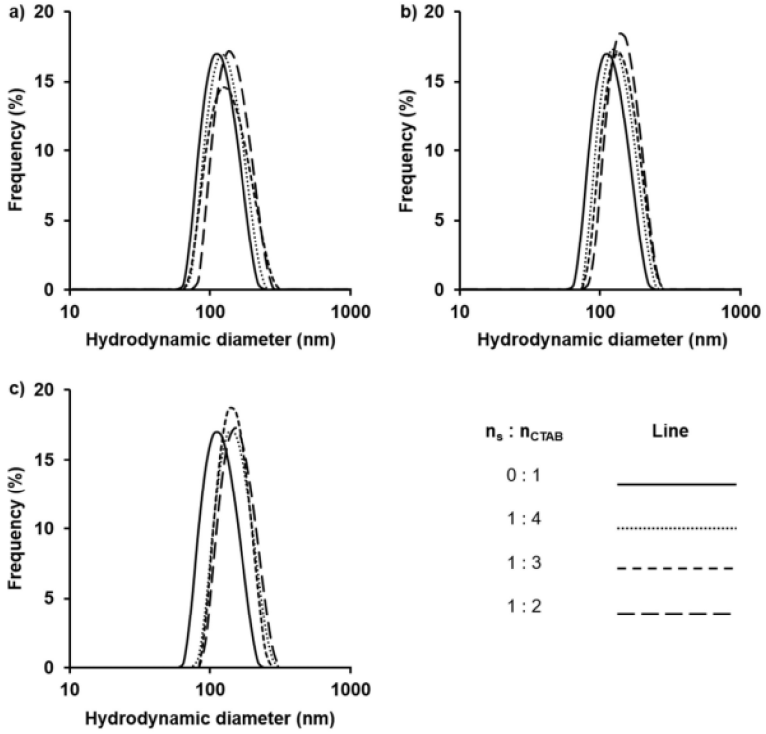

Figure 5.1. Size distribution by dynamic light scattering (DLS) measurement of a) $dSiO_2$@MSN-T20, b) $dSiO_2$@MSN-T80, and c) $dSiO_2$@MSN-BS10.

For each non-ionic surfactant, the mesoporous shell thickness gradually increased when its molar ratio with CTAB increased. This suggested that the higher the presence of non-ionic surfactants in the mixed micelle, the larger the mixed micelle diameter and the thicker the mesoporous shell. This phenomenon could be explained as follow: when the diameter of micelles used as co-templates of mesopore increased, the residual surface area as well as the space around the

$dSiO_2$ cores for the siloxane bridges to condense was narrowed, leading to the increase in the thickness of the mesoporous shell.

5.2. Effect of non-ionic surfactants on the mesopore diameter of $dSiO_2$@MSN

For further investigate the influence of non-ionic surfactants on mesopore diameter of HMSN, three synthesized $dSiO_2$@MSN samples using mixed micelles of T20, T80 or BS10 with CTAB at the molar ratio nS:nCTAB of 1:2 was determined their surface area and mesopore diameter (Figure 5.4).

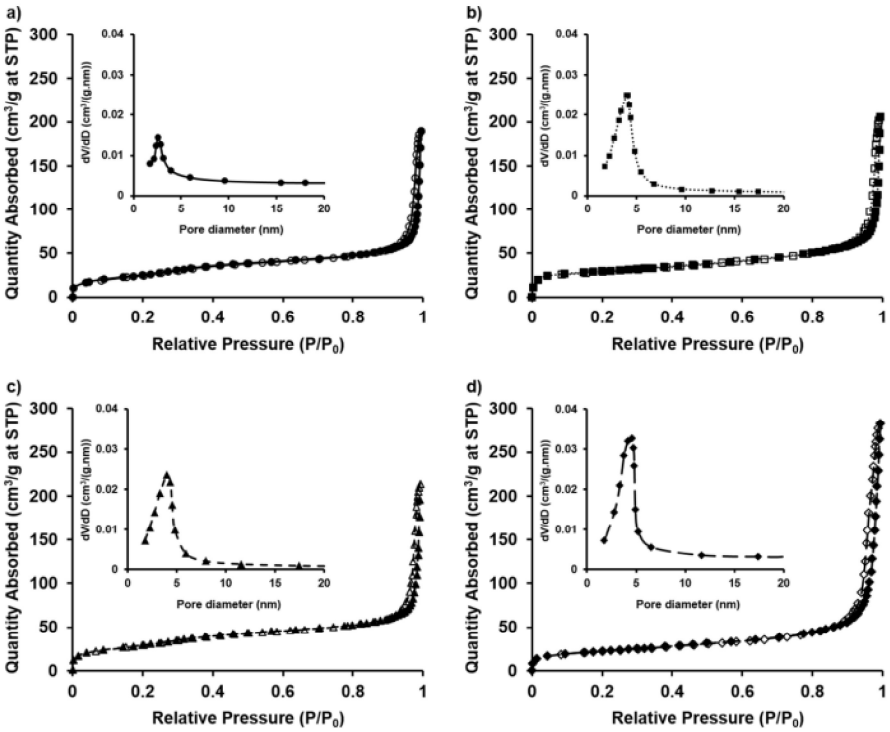

Figure 5.4. The N_2 adsorption-desorption isotherms and pore size distributions of a) $dSiO_2$@MSN, b) $dSiO_2$@MSN-T20, c) $dSiO_2$@MSN-T80 and d) $dSiO_2$@MSN-BS10.

According to IUPAC classification, the adsorption isotherms of the four samples were Langmuir type IV isotherm curve and type H_2 hysteresis loop. This type of pathway is characterized by mesoporous materials, suggesting that the presence of non-ionic surfactants in the mixed micelle during the mesoporous shell coating step did not change the nature of the nitrogen adsorption-desorption isotherms of the original particle. With the presence of the non-ionic surfactant in the micelle as soft template, the pore diameter significantly increased from 2.5 nm to more than 4.0 nm, of which, there was no notably different between the two samples $dSiO_2$@MSN-T20 and $dSiO_2$@MSN-T80 (4.1 nm and 4.0 nm), meanwhile $dSiO_2$@MSN-BS10 owned the biggest mesopores (4.5 nm).

Corresponding to the increase in pore diameter, the surface area of $dSiO_2$@MSN, $dSiO_2$@MSN-T20, $dSiO_2$@MSN-T80 and $dSiO_2$@MSN-BS10 samples were 67.2, 91.8, 92.2 and 106.7 m^2/g, respectively. To sum up, the influence of non-ionic surfactants on mesopore diameter and mesoporous shell thickness has been clarified.

5.3. Characterizations of the synthesized HMSNs

The synthesized HMSN particles with and without the presence of nonionic surfactants (at the molar ratio nS:nCTAB of 1:2) were characterized via SEM, TEM, particle size distribution and Zeta potential (Figure 5.5).

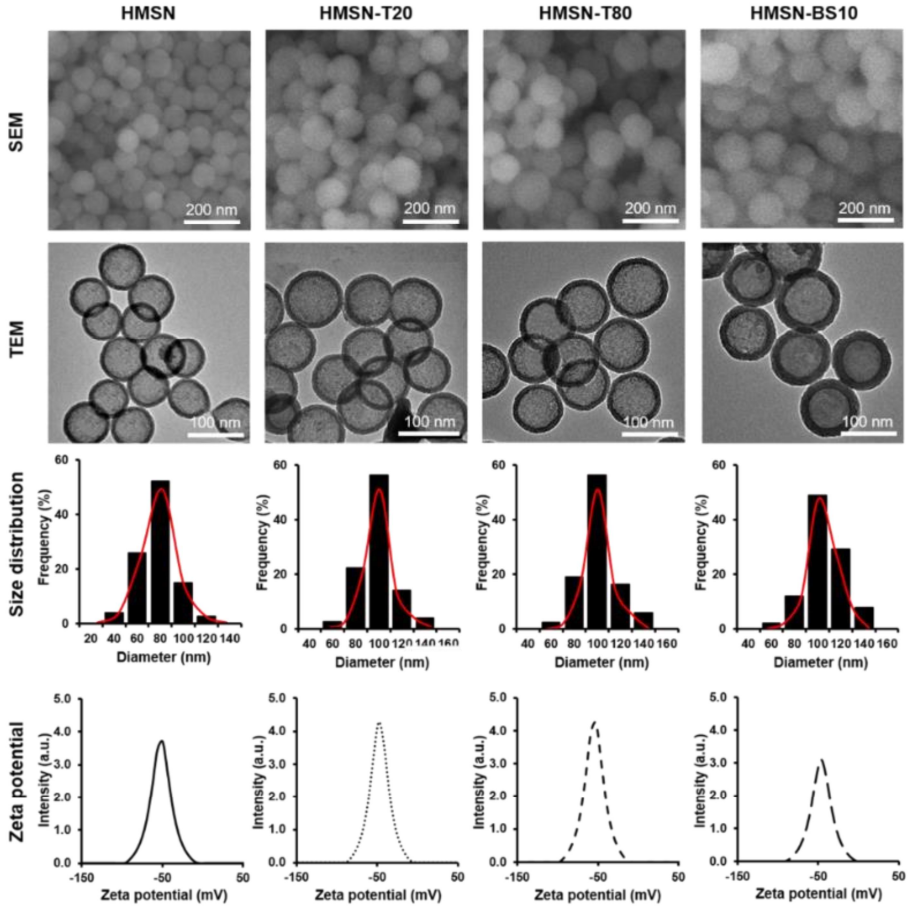

Figure 5.5. SEM images, TEM images, Size distribution and Zeta potential of HMSN, HMSN-T20, HMSN-T80 and HMSN-BS10.

As could be seen, all the synthesized samples were morphologically monodispersed spherical particles. SEM images confirmed the spherical, monodisperse and narrow size distribution with the particle diameter of HMSN, HMSN-T20, HMSN-T80 and HMSN-BS10 were 80.2, 99.3, 100.8 and 110.4 nm, respectively. Moreover, TEM images suggested that the synthesized HMSN with the presence of non-ionic surfactants remained its hollow@shell structure.

Additionally, zeta potential of the four samples HMSN, HMSN-T20, HMSN-T80 and HMSN-BS10 had negative values around -50 mV, indicating that CTAB and other non-ionic surfactants were well removed from the synthesized HMSNs.

5.4. Drug loading and in vitro drug release of the synthesized HMSNs

Rose Bengal with MW of 1017.64 g/mol (twice higher than that of DOX) was used as model drug. RB loading efficiency (DLE) and RB loading capacity (DLC) of HMSN, HMSN-T20, HMSN-T80 and HMSN-BS10 were measured and presented in Figure 5.7a. The results showed that both DLE and DLC values of HMSN were significant lower than those of HMSN-S. This might be due to the difference between the mesopore diameter and the cargo size.

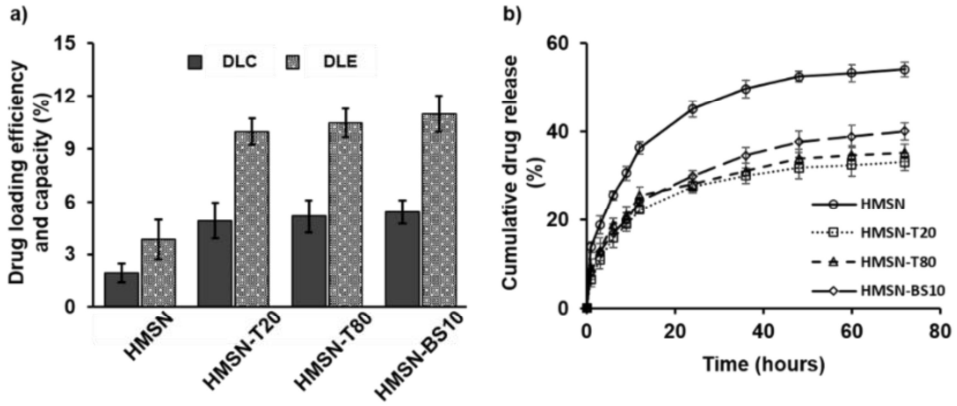

Figure 5.7. (a) Rose bengal (RB) loading capacity (DLC - grey) and loading efficiency (DLE - black) of HMSN, HMSN-T20, HMSN-T80 and HMSN-BS10; (b) In vitro release profile of RB from HMSN, HMSN-T20, HMSN-T80 and HMSN-BS10. The marked points correspond to 0, 1, 3, 6, 9, 12, 24, 36, 48, 60 and 72 h, respectively.

In the previous report, with DOX (MW of 543.52 g/mol and molecular size of 1.5 nm), HMSN (mesopore diameter of 2.5nm) performed relative good DLE and DLC values of 5.87% and 11.09%, respectively. In contrast, RB used in the current study had MW of 1017.64 g/mol, which was twice higher than that of DOX, would therefore own larger molecular size compared to DOX and be hard to pass through the mesopores of the original HMSN. The low values DLC and DLE of HMSN, defined as 1.95% and 3.82%, respectively, were thought to be mainly the amount of RB adsorbed on the surface of the particles. Meanwhile, thanks to the presence of non-ionic surfactants, the mesopore diameter of HMSN-T20, HMSN-T80 and HMSN-BS10 were enlarged up to more than 4.0 nm, leading to an easy passage of RB through the mesoporous channels and higher amount of cargos loaded inside the hollow cavity. The similarity of DLC and DLE between HMSN-T20 and HMSN-T80 was thought to be due to the fact that they had mesopores with similar diameters while HMSN-BS10 performed the best

DLE and DLC because it had the largest mesoporous channels (as presented in the BET and BJH results).

For the drug release profiles (Figure 5.7b), RB@HMSN-S showed their similarity in the cumulative amount of released drug over the time, suggesting better control release profiles compared to that of RB@HMSN. The burst release of RB@HMSN might be due to RB was absorbed on the surface but unloaded inside the particles. Meanwhile it took time for the loaded RB in RB@HMSN-S to be released from the hollow through longer meso-channel to the outside. Among the three systems RB@HMSN-S, RB@HMSN-BS10 showed slightly faster release profile compared to the others. This phenomenon was consistent with the largest mesopore diameter of HMSN-BS10 which was reported in the previous section.

In addition, FT-IR, XRD and MTT analyzes were performed to characterize and evaluate the biocompatibility of HMSN and HMSN-S particles.

-------o0o-------

CHAPTER 6. SURFACE MODIFICATION OF HOLLOW MESOPOROUS SILICA NANOPARTICLES WITH PLURONICS FOR DUAL DRUGS DELIVERY

6.1. Modification of HMSNs' surface with Pluronics

Pluronics with different number of hydrophilic PEO and hydrophilic PPO blocks including L64, F68 and F127 were used to modify the HMSN surface for dual drug delivery application of Doxorubicin (DOX) and Quercetin (QUE).

HMSN-Plu systems were proved to be successfully synthesized through Zeta potential, DLS, FT-IR and TGA analysis. Zeta potential of the three samples HMSN-L64, HMSN-F68 and HMSN-F127 were identified as 37.8 mV, 30.2 mV and 20.2mV, respectively (Figure 6.4a). They were all positive but lower than that of HMSN-NH_2. This could be due to the reaction between the activated Pluronics with amine groups on the surface of HMSN-NH_2, leading to a decrease in the amount of amine groups on the obtained nanoparticles' surface. There was a gradual increase in DLS size from 127.9 nm to 142.1 nm and 172.7 nm when HMSN particles were conjugated to Pluronics of increasing molecular weight (from 2900 kDa to 8400 kDa and 12600 kDa). This was thought to be due to the corresponding increase of the chain length of Pluronic molecules.

In Figure 6.4c, the FT-IR spectra of HMSN-Plu appeared the absorption signals of both naked HMSN particles by amine group (Figure 6.3c) and activated NPC-Plu-OH (Figure 6.1). The absorption peaks at 3300-3500 cm^{-1} and 1089 cm^{-1} corresponded to the -OH and Si-O-Si groups of the naked HMSN. Meanwhile, the three FT-IR spectra of HMSN-Plu also had absorption peaks at 2888 cm^{-1} and 1111 cm^{-1} which together attributed to the group -OCH_2-CH_2- of the Pluronics.

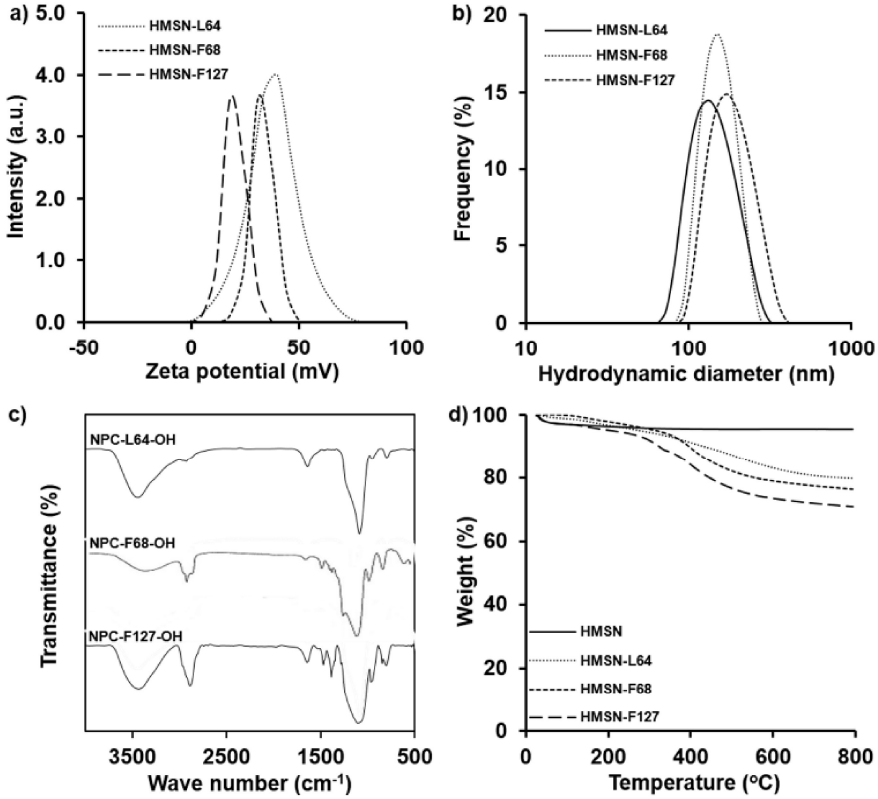

Figure 6.4. Characterizations of HMSN-L64, HMSN-F68 and HMSN-F127: a) Zeta potential; b) Hydrodynamic particle diameter; c) FT-IR spectra; and d) TGA graphs

Figure 6.4d showed the TGA graphs of HMSN and HMSN-Plu. The initial mass loss at temperature below 200 °C could be ascribed to the removal of humidity and to the condensation of surface silanols. Meanwhile, the loss of weight at temperature above 200 °C could be directly related to the extent of surface functionalization. From the TGA data, the weight loss values of HMSN and HMSN-Plu in the temperature ranges of 0-200 °C and 200-800 °C were determined, respectively, as 14.56, 17.61 and 19.05%, hence, could be ascribed to amount of the corresponding Pluronic modifying in the HMSNs' surface. TGA result, together with FT-IR, zeta potential and DLS results, demonstrated that the three Pluronics were successfully modified on the HMSNs' surface.

6.2. Dual drugs loading capacity and in vitro release behavior of HMSN-Plu

DOX and QUE were respectively encapsulated into the conventional HMSN and the modified HMSN-Plu. Their loading capacity and loading efficiency were presented in Table 6.2 as follow:

Table 0.1. Loading capacity (DLC) and loading efficiency (DLE) for Doxorubicin (DOX) and Quecertin (QUE) of HMSN and HMSN-Plu

Particles	DLC (%)		DLE (%)	
	DOX	QUE	DOX	QUE
HMSN	5.87 ± 0.64	2.34 ± 1.03	15.15 ± 0.94	9.60 ± 0.78
HMSN-L64	7.04 ± 0.81	9.80 ± 1.16	19.88 ± 1.02	43.44 ± 1.18
HMSN-F68	6.79 ± 0.59	9.83 ± 0.79	19.28 ± 0.87	43.82 ± 1.05
HMSN-F127	6.97 ± 0.97	17.80 ± 0.85	19.50 ± 1.13	86.83 ± 0.98

The loading capacity for DOX of the three samples HMSN-Plu slightly increased compared to that of HMSN. The difference could be due to the ability of DOX to bind with the remaining amine groups on the HMSN-Plu surface via imine forming reaction. Meanwhile, there was a clearly noticeable difference between QUE loading capacity values among the samples. HMSN owned the lowest DLC value (2.34%), HMSN-L64 and HMSN-F68 showed better loading capacity for QUE with DLC value of 9.80% and 9.83%, respectively, meanwhile HMSN-F127 performed the highest DLC values of 17.80%.

The relative similarity in DOX loading capacity of the samples was due to the fact that DOX was previously encapsulated, when the cavities and pores of the materials were empty. Thus, DOX, a hydrophilic drug, could reside in these empty spaces without any competition. QUE was then loaded into the DOX encapsulated materials. At this time, the remaining space inside the materials for QUE was not as much as for DOX. That was the reason why the DLC value for QUE of HMSN was the lowest. Fortunately, hydrophobic blocks PPO of the Pluronic molecules on HMSN-Plu's surface was the sites where QUE, a poorly soluble drug, could be effectively encapsulated through physical interaction, resulting in marked enhancement of QUE loading capacity of HMSN-Plu. When considering the structure of L64, F68 and F127, it was possible to find a correlation between QUE loading capacity and the number of PPO blocks. The more PPO units a Pluronic had, the higher QUE loading capacity a HMSN-Plu showed.

6.3. In vitro drug release behavior of HMSN-Plu

In vitro drug release behavior of free drugs and loaded drugs was investigated in different conditions including [37 ^{o}C, pH 7.4], [18 ^{o}C, pH 7.4] and [37 ^{o}C, pH 5.5]. The results were showed in Figure 6.5.

For DOX release, at the three conditions, free DOX was released the fastest, followed by DOX from HMSN, whereas HMSN-Plu showed better controlled DOX release profiles. This proved that the modified Pluronics on HMSNs' surface had come into play as the caps to reduce the opening of the mesoporous

channels, slowing down the movement of DOX from the hollow cavity out to the environment.

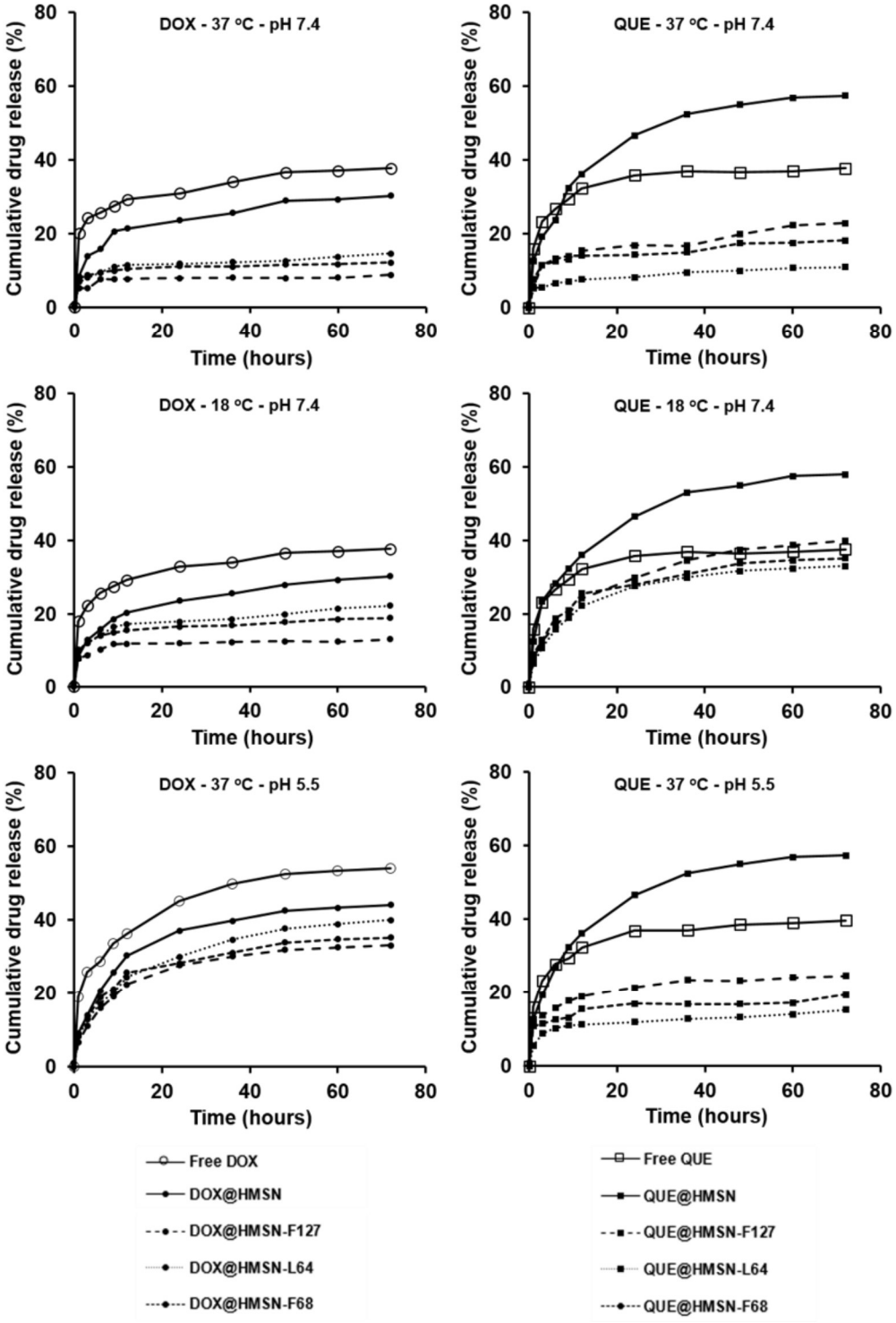

Figure 6.5. In vitro release behaviour of free drugs and loaded drugs in different conditions of temperatures and pH values

After 72 h, although the released DOX amount from HMSN-Plu samples increased when the temperature reduced from 37 to 18 ^{o}C (at the same pH value of 7.4), the differences were not significant. Meanwhile, there were notable increases in the amount of cumulative DOX release after 72 h at pH 5.5. This phenomenon was attributed to the dimerization of DOX in PBS pH 7.4 where DOX interacted with the buffer and formed covalently bonded DOX dimers. The results suggested that the three HMSN-Plu systems released DOX in response to pH, in which HMSN-Plu systems performed slow DOX release rates in physiological condition and higher rates in tumor microenvironment condition.

For QUE release, HMSN showed burst release profiles at all tested conditions. This was due to the loaded QUE was mainly adsorbed on the HMSNs'surface. Meanwhile, the drug release rate (%) was calculated as the percentage of cumulative released drug with the loaded drug. Therefore, although HMSN showed high percentages of drug released, the absolute mass of drug released was very small. Free QUE and loaded QUE from HMSN-Plu were released more slowly than those from HMSN. This could be due to the high initial amount of QUE (free or loaded in the materials) and its poor solubility. This is an advantage of the HMSN-Plu loading QUE systems because they can limit the leakage of QUE when circulating in the body under the physiological condition. Besides, HMSN-Plu also showed improvement in drug release rate at low temperature (18 ^{o}C). This phenomenon could be explained by the stretching of Pluronic chains at low temperature, causing the encapsulated QUE molecules in the hydrophobic PPO blocks to be released easily out to the environment by the concentration difference. The results suggested that the three HMSN-Plu systems released QUE in response to temperaure, in which HMSN-Plu systems performed slow QUE release rates in physiological temperature and higher rates at cooler temperatures.

6.4. Characterizations of the HMSN-F127

The HMSN-F127 system is compared with HMSN through TEM, BET and XRD experiments. TEM images showed that both HMSN and HMSN-F127 were spherical monodisperse particles (Figure 6.8). The particle diameters of HMSN and HMSN-F127 were determined as 80.2 nm and 119.7 nm, respectively. The particles HMSN-F127 with such an appropriate size could not only load a sufficient amount of drug, but also prolong the circulation time during the administration.

The isotherms of N_2 adsorption–desorption and the distributions of pore diameter were shown in Figure 6.9. In addition, the large hysteresis loops in the relative pressure range (P/P0) of 0.5–1.0 suggested the hollow structure of the two particle systems. HMSN possessed a higher BET surface area (767 m^2/g)

compared to that of HMSN-F127 (446 m^2/g). Moreover, even though the pore diameters of HMSN and HMSN-F127 were similar (2.5 and 2.2 nm, respectively), dV/dD value of HMSN was significantly higher than that of HMSN-F127. The decrease of BET surface area and BJH pore volume of HMSN-F127 was due to the fact that F127 molecules presented on HMSNs' surface and acted as capping agents of the open pores.

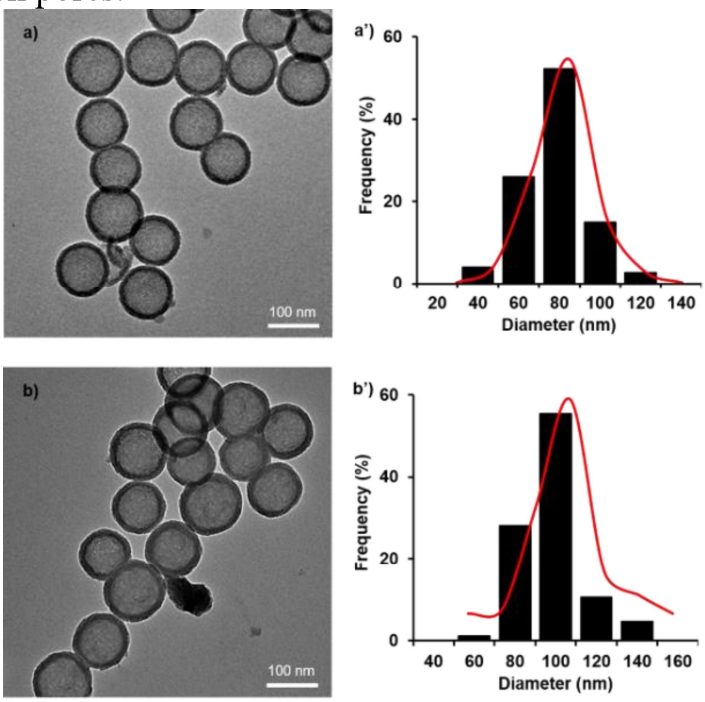

Figure 6.8. TEM images and Size distribution of a), a') HMSN and b), b') HMSN-F127

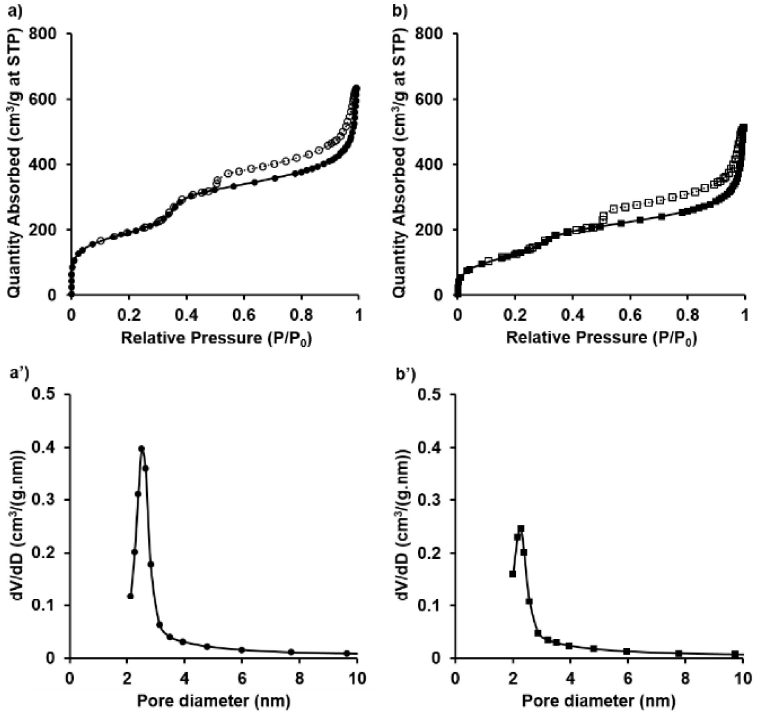

Figure 6.9. The N_2 adsorption-desorption isotherms and pore size distributions of HMSN (a, a') and HMSN-F127 (b, b')

6.5. Cancer cell killing ability of DOX.QUE@HMSN-Plu

In vitro cancer cell killing ability of free DOX, free QUE and DOX.QUE@HMSN-F127 against Hela cells was evaluated and presented in Figure 6.11. Overall, the free DOX, free QUE and DOX.QUE@HMSN-F127 samples induced cell death in concentration-dependent manners. Free QUE showed the lowest cytotoxicity on Hela cells with IC50 value of 3.29 µg/mL, while free DOX killed 50% of the cultured Hela cells at the concentration of 0.07 µg/mL. DOX.QUE@HMSN-F127 performed the strongest effect on the cells. The IC50 of DOX in DOX.QUE@HMSN-F127 was identified as 0.03 µg/mL, which was as half as that of free DOX. Although DOX was released at a slower rate from the nanocarrier HMSN-F127, the system simultaneously released QUE, which was proved to reduce the required dose as well as the side effect of DOX. That's the reason why the system DOX.QUE@HMSN-F127 showed the best cancer killing effect against Hela cells.

In addition, XRD and MTT analyzes were performed to characterize and evaluate the biocompatibility of HMSN and HMSN-Plu particles.

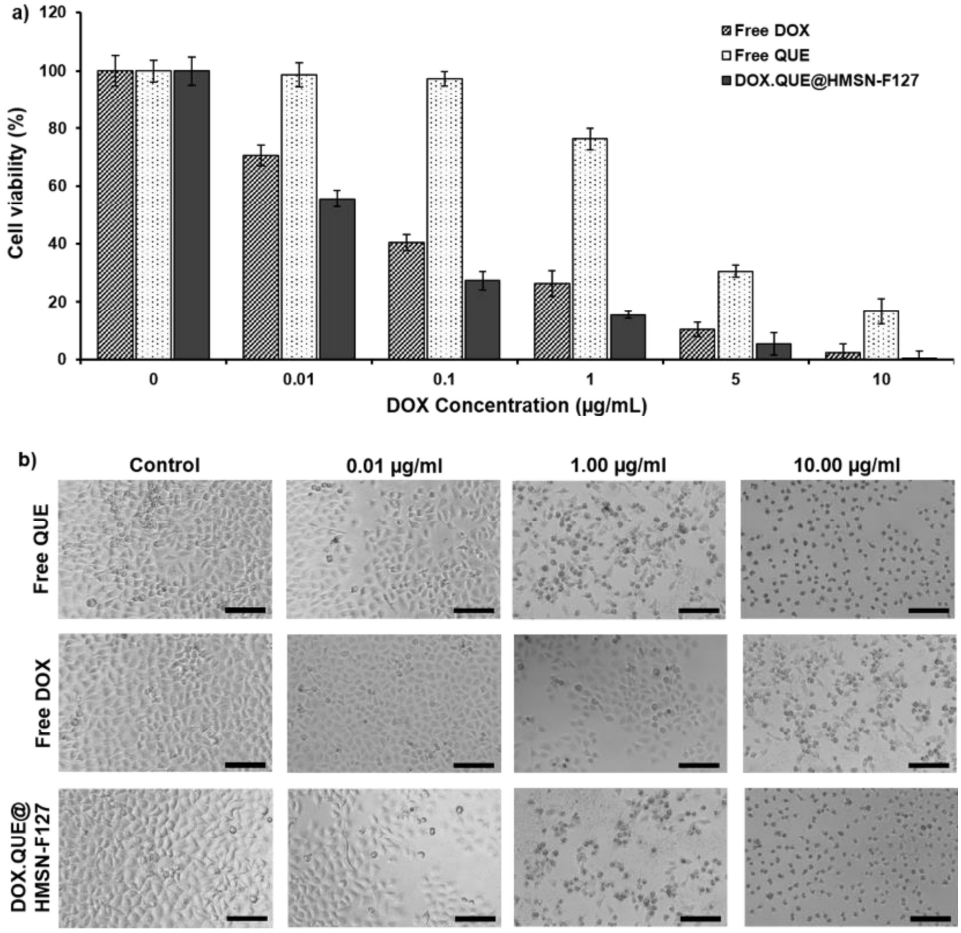

Figure 6.11. a) Cell viability and b) Mophorlogy of Hela cells treated by Free DOX, Free QUE and DOX.QUE@HMSN-F127. Scale bar is 100 µm

-------o0o------

CONCLUSIONS AND FUTURE PPROSPECS

To sum up, the current project has completed the set objectives. HMSN materials were firstly synthesized by hard-templating with shortened synthetic time and optimal particle size, secondly modulated mesoporous shell thickness and mesopore diameter, and finally surface modified with Pluronics for anti-cancer drugs delivery applications. In detail:

- The synthesis method of HMSN was successfully modified to shorten the synthetic time by more than half from 21 hours to 9 hours and reduce the HMSN particle size to about 80 nm.
- Mesoporous shell thickness of HMSN was successfully controlled using polyethylene glycol (PEG) in the shell coating step. As the molecular weight (1000, 2000, 4000 and 6000 Da) or concentration (1, 2, 3, 4 and 5%) of PEG increased, the shell thickness tended to increase. HMSN-P synthesized in the

presence of 2% PEG 6000 has a particle diameter of 94.3 nm and a mesoporous shell thickness of 14.5 nm, showing a slightly lower DOX loading capacity but a better controlled DOX release profile than the original HMSN.

- Mesopore diameter of HMSN was successfully controlled using non-ionic surfactants (Tween 20, Tween 80 and Brij S10) as co-templates for mesopores in the shell coating step. For each non-ionic surfactant, as the molar ratios S : CTAB increased, the mesoporous shell thickness of HMSN gradually increased. HMSN-T20, HMSN-T80 and HMSN-BS10 synthesized at the molar ratio S : CTAB of 1:2, respectively owned the enlarged mesopore diameters of 4.1, 4.0 and 4.5 nm, performing significantly higher loading capacity and better release controllability for Rose Bengal - a high molecular weight agent, compared to the original HMSN.
- Three types of Pluronics including L64, F68 and F127 were successfully modified on HMSNs' surface. The obtained HMSN-Plu systems significantly enhanced loading capacity as well as release controllability for DOX and QUE. HMSN-F127 showed great loading capacity with 6.97% for DOX and 17.8% for QUE. Moreover, HMSN-Plu showed good release controllability with temperature responsive release for QUE and pH responsive release for DOX.
- HMSN, HMSN-P, HMSN-S and HMSN-Plu were biocompatible nanocarriers with no observed cytotoxicity at concentrations up to 250 μg/mL, proved by MTT assays. Moreover, the great inhibition activity against human cervical cancer Hela cell line of the dual drug loading system DOX.QUE@HSMN-F127 was illustrated with IC50 value for DOX of 0.03 μg/mL, which was as half as that of free DOX.

-------o0o-------

THE NOVELTY OF THE THESIS

The hard-template synthesis method of HMSN was successfully modified to reduce the particle size below 100 nm with shortened synthetic time.

PEG with different molecular weights and concentrations were investigated and used as capping agent in the shell coating step to control the mesoporous shell thickness of HMSN.

Mixed micelles of non-ionic surfactants and CTAB were investigated and used as soft templates in the shell coating step to enlarged the mesopore diameter of HMSN.

Pluronic with different numbers of PPO and PEO units were used to modify the surface of HMSN particles for dual drug loading application. The loading capacity of drug with different solubility (DOX and QUE) as well as the drug release profile in response to temperature and pH of the HMSN-Plu systems were evaluated to select the most effective dual drug delivery HMSN-Plu system.

LIST OF WORKS PUBLISHED

1. Ngoc Hoi Nguyen, Cuu Khoa Nguyen, Dai Hai Nguyen, *"A Modified Hard-Templating for Hollow Mesoporous Silica Nanoparticles Synthesis with Suitable Particle Size and Shortened Synthesis Time"*, Vietnam Journal of Science and Technology, ISSN 2525-2518, 0866-708X, Accepted 20 August 2022.

2. Ngoc Hoi Nguyen, Dieu Linh Tran, Ngoc-Hang Truong-Thi, Cuu Khoa Nguyen, Dai Hai Nguyen, "*Simply and Effectively Control the Shell Thickness of Hollow Mesoporous Silica Nanoparticles by Polyethylene Glycol for Drug Delivery Applications"*, Journal of Applied Polymer Science, SCIE/SSCI, Q2, H index 175, IF 3.125, ISSN 0021-8995 (print); 1097-4628 (web). First published: 17 September 2022. DOI: http://doi.org/10.1002/app.53126.

3. Ngoc Hoi Nguyen, Ngoc-Hang Truong-Thi, Dinh Tien Dung Nguyen, Yern Chee Ching, Ngoc Trinh Huynh, Dai Hai Nguyen, *"Non-ionic Surfactants as Co-Templates to Control the Mesopore Diameter of Hollow Mesoporous Silica Nanoparticles for Drug Delivery Applications"*, Colloids and Surfaces A: Physicochemical and Engineering Aspects, SCIE/SSCI, Q2, H index 179, IF 5.518, ISSN 0927-7757, Received 27 July 2022, Revised 30 August 2022, Accepted 19 September 2022, Available online 21 September 2022, Version of Record 22 September 2022. DOI: https://doi.org/10.1016/j.colsurfa.2022.130218

4. Ngoc Hoi Nguyen, Dai Hai Nguyen, *"A Research on Drug Delivery System based on Mesoporous Silica Nanoparticles for Anti-Cancer"*, The International Chemistry and Its Applications Conference 2022.